Monthly Notices of the ROYAL ASTRONOMICAL SOCIETY

MNRAS **529,** 556–562 (2024) https://doi.org/10.1093/mnras/stae431
Advance Access publication 2024 February 9

HD 12098: a highly distorted dipole mode in an obliquely pulsating roAp star

D. W. Kurtz [1,2★] H. Saio,[3] D. L. Holdsworth [2,4] Santosh Joshi[5] and S. Seetha[6]

[1]*Centre for Space Research, North-West University, Dr Albert Luthuli Drive, Mahikeng 2735, South Africa*
[2]*Jeremiah Horrocks Institute, University of Central Lancashire, Preston PR1 2HE, UK*
[3]*Astronomical Institute, Graduate School of Science, Tohoku University, Sendai 980-8578, Japan*
[4]*South African Astronomical Observatory, P.O. Box 9 Observatory, 7935 Cape Town, South Africa*
[5]*Aryabhatta Research Institute of Observational Sciences, Nainital 263001, Uttarakhand, India*
[6]*Raman Research Institute, C.V. Raman Avenue, Bengaluru 560080, India*

Accepted 2024 February 8. Received 2024 February 7; in original form 2023 December 18

ABSTRACT

HD 12098 is a rapidly oscillating Ap star pulsating in the most distorted dipole mode yet observed in this class of star. Using *Transiting Exoplanet Survey Satellite* (*TESS*) Sector 58 observations, we show that there are photometric spots at both the magnetic poles of this star. It pulsates obliquely primarily in a strongly distorted dipole mode with a period of $P_{\rm puls} = 7.85$ min ($\nu_{\rm puls} = 183.34905\,{\rm d}^{-1}$; 2.12210 mHz) that gives rise to an unusual quadruplet in the amplitude spectrum. Our magnetic pulsation model cannot account for the strong distortion of the pulsation in one hemisphere, although it is successful in the other hemisphere. There are high-overtone p modes with frequencies separated by more than the large separation, a challenging problem in mode selection. The mode frequencies observed in the *TESS* data are in the same frequency range as those previously observed in ground-based Johnson *B* data, but are not for the same modes. Hence the star has either changed modes, or observations at different atmospheric depth detect different modes. There is also a low-overtone p mode and possibly g modes that are not expected theoretically with the >1 kG magnetic field observed in this star.

Key words: asteroseismology – stars: chemically peculiar – stars: individual: TIC 445543326; HD 12098 – stars: oscillations.

1 INTRODUCTION

Magnetic peculiar A (Ap) stars are found in the main-sequence band from spectral types early-B to mid-F. They have global magnetic fields that are roughly dipolar with strengths up 34 kG and with a magnetic axis that is inclined to the rotation axis, so that the field is observed from varying aspect with rotation. Atomic diffusion gives rise to surface abundance anomalies that can reach a million times that of normal stars for some rare Earth elements. Those enhanced abundances are concentrated in surface patches, usually referred to as spots, that are closely associated with the magnetic poles, giving rise to rotational variations in the spectral line strengths (hence abundances) and in brightness. These stars are known as α^2 CVn stars; they constitute about 10 per cent of all main-sequence stars in that spectral type range.

A notable characteristic of the α^2 CVn stars is that the surface spots are stable over time-scales of at least decades, in strong contrast to lower main-sequence spotted stars for which those spots can evolve on time-scales of days. The Sun is the prime example of this. This stability in the Ap stars means that the rotational light curves can be used to determine the rotation period to high precision. While the spots are stable, they have a wide variety of surface configurations, often giving rise to non-sinusoidal light curves. When the rotational inclination, i, and the magnetic obliquity, β, of the dipolar field sum to greater than 90°, both magnetic poles are seen; also, when there are spots associated with both poles, the rotational light curve has a double wave.

The rapidly oscillating Ap (roAp) stars are a subset of the magnetic Ap stars that show high radial overtone p-mode pulsation with periods in the range 4.7–23.6 min (see Holdsworth et al. 2024). The spectral types of the roAp stars range from early A to late F with effective temperatures of $6500\,{\rm K} \leq T_{\rm eff} \leq 8800\,{\rm K}$. They partially overlap with the δ Sct stars in the Hertzsprung-Russell (HR) diagram, but differ from those because of the impact of the magnetic field on the pulsations. The roAp stars generally pulsate in non-radial, zonal dipole, and quadrupole modes ($l = 1, 2$; $m = 0$) with the pulsation axis lying close to the magnetic axis. This gives rise to oblique pulsation where the pulsation mode is seen from varying aspect as the star rotates. That provides information on the mode geometry, hence constrains mode identification, which in many other stars can be problematic. Mode identification is requisite for the application of asteroseismic modelling.

The oblique pulsator model was introduced by Kurtz (1982) and further developed and improved by Shibahashi & Saio (1985), Shibahashi & Takata (1993), Takata & Shibahashi (1994, 1995), Bigot & Dziembowski (2002), and Bigot & Kurtz (2011), among others. For pulsation modes that can be described by single spherical

★ E-mail: kurtzdw@gmail.com

harmonics, the pulsation amplitude and phase changes that are observed over the rotation cycle allow the oblique pulsator model to give constraints on i and β, thus on the pulsation geometry, hence identifying the mode. Two well-studied cases, HR 3831 and HD 99563, pulsate in slightly distorted dipole modes for which the rotational pulsation amplitude and phase modulation provide good constraints on the pulsation geometry (Kurtz, Shibahashi & Goode 1990, Handler et al. 2006).

Observations show that in other roAp stars the modes are often more strongly distorted. Saio (2005) made a non-adiabatic analysis of non-radial pulsation modes in the presence of a dipole field for roAp stars, finding that the dipole and quadrupole modes distorted by the magnetic field are most likely to be excited. Several cases of strongly distorted quadrupole modes were studied by Holdsworth et al. (2018, and references therein) and modelled with the method of Saio (2005). This was particularly successful in explaining the flattening of the pulsation phase curve as a function of rotation phase.

However, the models are not fully capable of explaining the distortion of the pulsation modes, and further complications and challenges to the oblique pulsator model, as applied to the roAp stars, have arisen. In particular, Kurtz & Holdsworth (2020) showed that the geometry deduced for the dipole pulsation mode in the roAp star HD 6532 is dramatically different for observations made in Johnson *B* and for those made with the red-dominated bandpass of the *Transiting Exoplanet Survey Satellite* (*TESS*) mission. Since observations at these different wavelengths probe to different atmospheric depths because of differences in opacity, this suggests strong changes in pulsation geometry as a function of depth. In a high-resolution spectroscopic study of the distorted dipole mode in HR 3831, Kochukhov (2006) first pointed out that the pulsation geometry inferred using the oblique pulsator model is dependent on the depth of the observations.

Hence the roAp stars continue to present challenges to our understanding of their oblique pulsation. This is particularly true for the stars with the most distorted mode geometries. This has recently become relevant in the context of the tidally tilted pulsators, where tidally distorted zonal and sectoral dipole modes have been observed (Fuller et al. 2020; Handler et al. 2020; Kurtz et al. 2020; Rappaport et al. 2021; Jayaraman et al. 2022). Thus the study of oblique pulsation of distorted non-radial modes has expanding applications. Therefore, in this work, we present the most distorted dipole mode yet observed in an roAp star. Extreme examples provide the strongest challenges to theory.

1.1 HD 12098

HD 12098 has only one published spectral classification, which is F0 from the original HD catalogue. However, its Strömgren colours and indices are characteristic of cool Ap stars; $b - y = 0.191$, $m_1 = 0.328$, $c_1 = 0.517$, H $\beta = 2.796$ (Olsen 1983), from which the indices $\delta m_1 = -0.122$, and $\delta c_1 = -0.255$ can be calculated from the calibration of Crawford (1979). Based on these indices, in 1999 the star was tested for pulsation under the Nainital-Cape Survey project (Ashoka et al. 2000; Martinez et al. 2001; Joshi et al. 2006, 2009, 2016) using 10-s integrations through a Johnson *B* filter on the 1.04-m Sampurnanand telescope of the Aryabhatta Research Institute of Observational Sciences (at that time called the Uttar Pradesh State Observatory). Martinez et al. (2000) found it to be an roAp star with a pulsation frequency of 189.2 d^{-1} (2.19 mHz; $P = 7.6$ min).

Girish et al. (2001) then obtained further data from Mt. Abu Observatory, India, and found the star to be multiperiodic with a dominant frequency of 187.82 d^{-1} (2.17 mHz). They also found rotational variation, but could not discriminate between periods of 1.2 and 5.5 d. That ambiguity was addressed by Wade et al. (2001) and then resolved by Ryabchikova et al. (2005) who found a rotation period of 5.460 ± 0.001 d from a study of the mean longitudinal field, which varies almost sinusoidally between +2000 and −500 G with that period. That shows that both magnetic poles are seen over the rotation cycle.

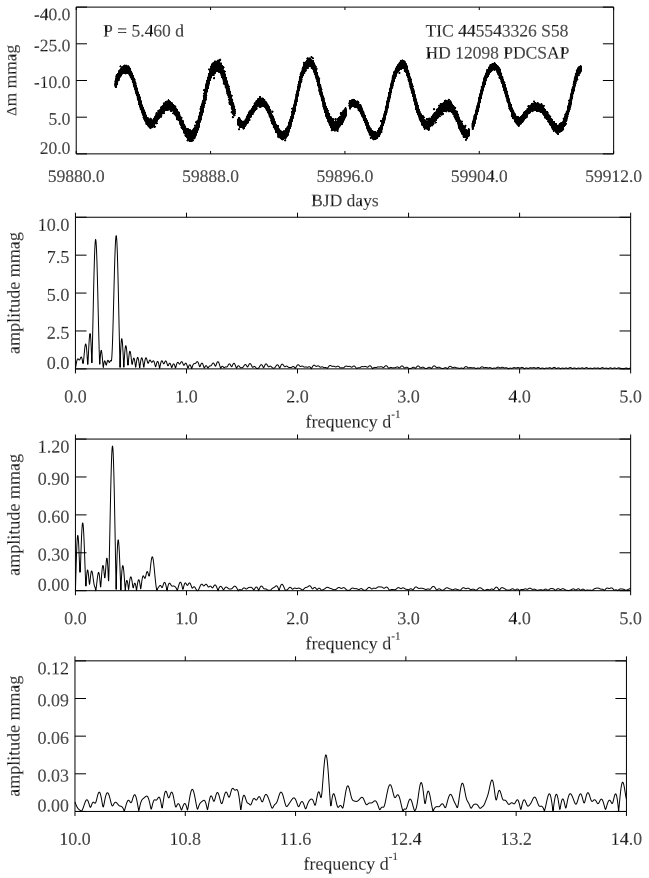

Figure 1. Panel 1: the Sector 58 *TESS* light curve for HD 12098 showing the double-wave rotational variation typical of the α^2 CVn stars. Panel 2: a low-frequency amplitude spectrum showing the first two harmonics of the rotation frequency. Panel 3: a low-frequency amplitude spectrum after pre-whitening a 10-harmonic fit for the rotation frequency. There are significant peaks visible that may be from g modes. One of these is not fully resolved from the second harmonic of the rotation frequency. Panel 4 shows a 5σ peak that is potentially from a low-order p mode. Note the changes of ordinate scale on the panels.

2 HD 12098 DATA AND ANALYSIS

HD 12098 was observed at 120-s cadence by the *TESS* mission in Sector 58 in late 2022. We have used the PDCSAP (Presearch-Data Conditioning Simple Aperture Photometry) data to study the rotation and pulsation variations of this star. The data span 27.72 d and comprise 19 475 data points. No outliers were removed.

2.1 The rotation period

Fig. 1 shows the Sector 58 light curve in the top panel showing a clear double wave. This is consistent with polar spots and the longitudinal magnetic field curve of Ryabchikova et al. (2005). The second panel shows the first two harmonics of the rotational light variation in an

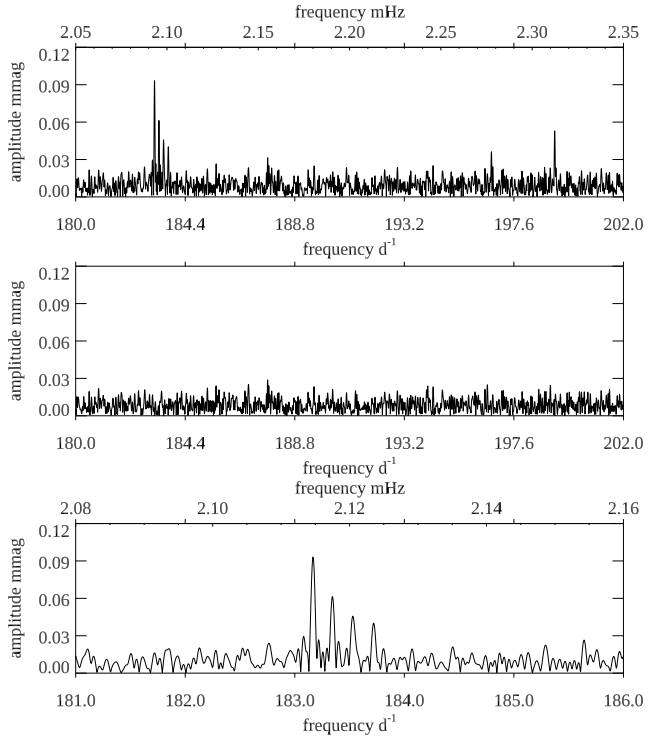

Figure 2. Panel 1: the roAp pulsation frequencies. Panel 2: same as panel 1 after pre-whitening the six pulsation frequencies. Panel 3: a higher resolution view of the 183.3491 d^{-1} (2.1221 mHz) rotational multiplet.

amplitude spectrum calculated using the Discrete Fourier Transform algorithm of Kurtz (1985). The rotation period determined from those harmonics is 5.4815 ± 0.0002 d, which is significantly different to that determined from the magnetic variation by Ryabchikova et al. (2005) of 5.460 ± 0.001 d.

After fitting 10 harmonics of the rotation frequency, the third panel of Fig. 1 shows significant peaks that may indicate some g modes. One of these is not fully resolved from the second harmonic of the rotation frequency, hence may have perturbed the value of the rotation period determined. Panel 4 shows a 5σ peak at 11.819 d^{-1} that is potentially from a low-overtone p mode. Because of this possible perturbation of the rotation frequency by an unresolved g-mode frequency, we adopt the rotation period (frequency) of $P_{\rm rot}$ = 5.460 d ($\nu_{\rm rot}$ = 0.183) of Ryabchikova et al. (2005) for the pulsation analysis. Pre-whitening by a 10-harmonic series with this rotation frequency provides a good fit to the data.

2.2 The pulsations

A high-pass filter was used to remove the low-frequency rotational frequency and its harmonics, the (probable) g-mode and p-mode frequencies, and instrumental variations so that the noise in the amplitude spectrum is white. This gives the best uncertainty estimates for the derived roAp pulsation frequencies, amplitudes, and phases. The top panel of Fig. 2 shows a section of the amplitude spectrum in the range of the roAp pulsation frequencies where six significant peaks can be seen, four of which form a quadruplet split by exactly the rotation frequency. The middle panel shows the amplitude spectrum of the residuals after those six frequencies were pre-whitened. The bottom panel shows a higher resolution view of the quadruplet. Table 1 gives the frequencies derived from a least-squares fits of

Table 1. A linear least-squares fit of the frequencies derived from the Sector 58 data for HD 12098. The zero-point for the phases is t_0 = BJD 2459893.80, which matches the time of magnetic maximum predicted from the ephemeris of Ryabchikova et al. (2005). The second frequency of the quadruplet, ν_2 = 183.3491 d^{-1} (2.1221 mHz) is taken to be the mode frequency from a distorted dipole. The other two frequencies are assumed to be from independent pulsation modes, for which there is no sign of rotational sidelobes as expected for oblique pulsation; those, if present, could be lost in the noise. The frequencies ν_1 to ν_4 are overspecified to five decimals so that it can be seen that they are exactly equally split by 0.18315 d^{-1} ($P_{\rm rot}$ = 5.460 d).

	Frequency (d^{-1})	Amplitude (mmag) ±0.007	Phase (rad)
ν_1	183.16590 ± 0.00141	0.098	0.190 ± 0.070
ν_2	183.34905	0.061	2.303 ± 0.114
ν_3	183.53220	0.047	−2.056 ± 0.148
ν_4	183.71535	0.040	−2.443 ± 0.173
ν_5	196.6986 ± 0.0040	0.035	1.470 ± 0.200
ν_6	199.2402 ± 0.0025	0.054	−1.832 ± 0.128

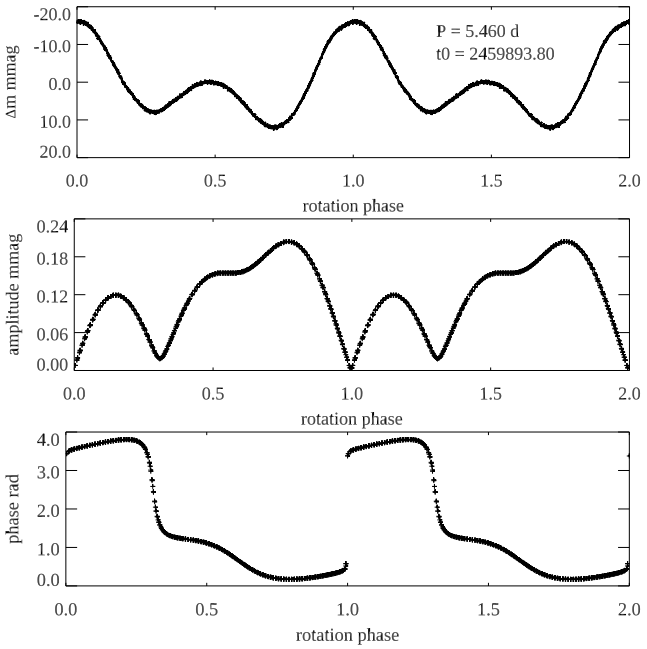

Figure 3. Panel 1: the Sector 58 *TESS* light curve phased; the data have been binned by 10. Panels 2 and 3: the pulsation amplitude and phase as a function of rotation phase. These have been calculated from the frequency quadruplet only, with ν_2 = 183.34905 d^{-1} as the mode frequency.

the quadruplet with a forced splitting equal to the rotation frequency, and the other two pulsation frequencies.

Fig. 3 shows the rotational light variations and pulsation amplitude and phase as a function of rotation phase. The time zero-point, t_0 = BJD 245 9893.80, was chosen to be the time of maximum rotational brightness. The pulsation amplitude and phase were calculated from the frequency quadruplet, taking ν_2 = 183.34905 d^{-1} (2.1221 mHz) to be the pulsation frequency, and the other three frequencies, ν_1, ν_3, and ν_4 to be rotational sidelobes generated by oblique pulsation. A noise-free time series was generated for this frequency quadruplet as given in Table 1, sampled at the times of the actual observations. The pulsation amplitudes and phases were then derived by least-squares fitting of the pulsation mode frequency, ν_2, to sections of the

generated data 0.05-d long, which is just over nine pulsation cycles. Those were then plotted as a function of rotation phase. The choice of ν_1 or ν_3 as the pulsation frequency generated pulsation phase plots, such as the bottom panel of Fig. 3, that had strong slopes, indicating that those are not the pulsation frequency.

2.3 Discussion of the pulsation frequencies

Several characteristics of the curves in Fig. 3 are notable. (1) The pulsation phase changes by π radians at the times when the pulsation amplitude goes to zero (or nearly so). This is a characteristic of an oblique dipole pulsation when the pulsation node crosses the line of sight. (2) One pulsation pole dominates for about 30 per cent of the rotation period and the other for about 70 per cent. This is consistent with the longitudinal magnetic curve of Ryabchikova et al. (2005), which shows the longitudinal magnetic field to be negative for about 30 per cent of the rotation and positive for the other 70 per cent. (3) The double-humped pulsation amplitude maximum between rotation phases 0.3 and 1.0 shows that the dipole mode is heavily distorted on this magnetic hemisphere of the star. The corresponding pulsation phase is also significantly distorted. (4) The pulsation amplitude and phase variation on the other magnetic hemisphere does not appear to be distorted. (5) The time of brightest light in the rotation curve coincides with the time of one pulsation minimum. This suggests that the star is brightest around the pulsation equator and dimmest near the poles, as is characteristic of α^2 CVn stars.[1] However, the pulsation mode is so distorted from a simple dipole, that this is a conjecture. (6) The mode frequency separation $\nu_6 - \nu_5 = 2.54\,\mathrm{d}^{-1}$ (29 μHz) is plausibly half the large separation, suggesting that these two modes are of alternatively even and odd degree, ℓ, and that the large separation is about $\Delta\nu_0 \sim 60$ μHz. (7) The other mode frequency separation $\nu_5 - \nu_2 = 13.350\,\mathrm{d}^{-1}$ (155 μHz) is then about 2.5 $\Delta\nu_0$, so that some intermediary modes are not excited to observable amplitude. This is seen in some other roAp stars, particularly, e.g. HD 217522 (Medupe et al. 2015).

The rotational variations in the mean longitudinal magnetic field shown in fig. 2 of Ryabchikova et al. (2005) shows that pulsation maximum occurs at the time of positive magnetic extremum. The magnetic ephemeris of Ryabchikova et al. (2005) cannot be meaningfully extrapolated across the nearly 20-yr time gap between the magnetic measurements and the *TESS* photometry to compare the time of pulsation maximum in the *TESS* data with then extrema of the magnetic field. Interestingly, fig. 2 of Ryabchikova et al. (2005) shows that the mean longitudinal magnetic field of HD 12098 is negative for 30 per cent of the rotation period and positive for 70 per cent. Those are the same percentages of the rotation period for which we see the two pulsation amplitude maxima in Fig. 3. We therefore conclude that the first pulsation maximum occurs when the negative magnetic hemisphere is observed, and the second, more complex maximum occurs when the positive magnetic hemisphere is visible. As with other roAp stars, it is likely that the pulsation amplitude maxima occur at the times of magnetic extrema, as appears to be the case in fig. 2 of Ryabchikova et al. (2005) for the Johnson *B* observations of Girish et al. (2001; see the next section). New contemporaneous magnetic and photometric observations are needed to confirm these reasonable conclusions.

There are no systematic studies of the pulsation amplitude and phase as a function of rotation phase, as shown in Fig. 3, compared to the rotational light curves in roAp stars. With *TESS* data, such a study would be useful.

2.4 Comparison with ground-based data

Observing through a Johnson *B* filter, Girish et al. (2001) obtained ground-based observations and found four pulsation frequencies in the range 187.7–198.7 d^{-1} (2.17–2.30 mHz). It is clear from comparison with Fig. 2 that peaks in this frequency range are not present in the *TESS* Sector 58 data, although $\nu_6 = 199.2402\,\mathrm{d}^{-1}$ (2.3060 mHz) is close. Similarly, the frequency quadruplet seen in Fig. 2 in the range 183.166–183.715 d^{-1} (2.120–2.126 mHz) is clearly not present in the Girish et al. (2001) data (see Fig. 5 in Section 3 below). As some roAp stars are known to have modes that show amplitude variation on time-scales as short as days, and others have been observed to change modes on longer time-scales, this may be the explanation for the different frequency ranges found in these two studies.

Alternatively, it is known that the pulsation amplitudes and phases in roAp stars vary strongly both as a function of atmospheric depth and over the surface as seen in the spectral lines of elements trapped in abundance spots, usually associated with the magnetic poles (see e.g. Kurtz, Elkin & Mathys 2006 and Freyhammer et al. 2009 for graphic examples). A theoretical study of magneto-acoustic modes as a function of atmospheric depth by Quitral-Manosalva, Cunha & Kochukhov (2018) provides insight into how the acoustic and Alfvén components of the modes vary throughout the line-forming layers of the observable atmosphere. It thus seems possible that mode observed by Girish et al. (2001) in Johnson *B* may have lower amplitudes, or be undetectable, in the deeper region observed by *TESS* with its red bandpass.

Yet, unexplained complexity in the roAp pulsation modes and in the application of the oblique pulsator model to those stars gives rise to uncertainty in the inference of geometrical information about those modes. Two examples are the suggested discovery of modes with two different pulsation axes in the roAp star KIC 10195926 (Kurtz et al. 2011), and the finding that the pulsation geometry inferred from application of the oblique pulsator model is very different in ground-based Johnson *B* data and *TESS* red data in the roAp star HD 6532 (Kurtz & Holdsworth 2020).

The measured photometric amplitudes of pulsation modes in roAp stars vary significantly depending on the bandpass used to make the observations (Medupe & Kurtz 1998) with amplitudes dropping from the blue to the red. This is simply a consequence of the spectral energy distribution and the photometric amplitude being primarily the result of temperature variations. Cunha et al. (2019) compared photometric amplitudes measured through Johnson *B* and *TESS* red bandpass for some roAp stars and found that measurements in Johnson *B* typically show about six times the amplitude of measurements in *TESS* red. However, there is also an atmospheric depth effect, since photometric observations in different bandpasses sample different atmospheric depths, on average. Given the strong dependence of pulsation amplitude on atmospheric depth, it is not possible to conclude whether HD 12098 has changed modes between the time of the ground-based Johnson *B* observations and the *TESS* observations, or whether the detected modes have very different amplitudes when observed through different bandpasses. Simultaneous observations

[1]The rotational photometric maximum and minimum in Ap stars is a function of the bandpass used for the observations. For some stars the maximum in a blue bandpass coincides with the minimum in a red bandpass. This is a consequence of the observations sampling different atmospheric depths and the line blocking from enhanced abundances changing the temperature gradient.

Table 2. Adopted parameters of HD 12098.

Parallax = 6.833 ± 0.022 mas, $T_{\rm eff}$ = 7600 K	[a]
V = 7.97 mag, $E(B-V)$ = 0, BC = 0.	[b]
$M_{\rm V}$ = 2.14 mag, log(L/L$_\odot$) = 1.04, log$T_{\rm eff}$ = 3.881	[c]

[a]GAIA DR3: Gaia Collaboration (2016, 2023).
[b]Netopil et al. (2008).
[c]log means logarithm of base 10.

in multiple bandpasses, including Johnson B, and with *TESS* are needed to discriminate between these possibilities.

3 MODELLING

In this section, we model the pulsational amplitude and phase modulations against rotational phase of the main p-mode pulsation of HD 12098 (middle and bottom panels of Fig. 3). We obtain these modulations by integrating the eigenfunction of the p mode on the visible hemisphere at each rotational phase for an assumed set of angles β and i; the angle between rotational/magnetic axes and the inclination angle of the line of sight against the rotation axis, respectively (Saio & Gautschy 2004; Holdsworth et al. 2016). We assume the limb-darkening parameter $\mu = 0.6$ in this paper.

The pulsational eigenfunctions are calculated by taking into account the effect of a dipole magnetic field (Saio 2005) with strength specified by the field strength $B_{\rm p}$ at the magnetic poles. Non-adiabatic pulsation variables (assumed to be axisymmetric to the magnetic axis neglecting rotation effects) are represented as a sum of the terms proportional to the Legendre function $P_{\ell_j}(\cos\theta)$ with $\ell_j = \ell_0 + 2j$ where $j = 1, 2, \ldots j_{\rm max}$ ($\ell_0 = 0$ for even modes and $\ell_0 = 1$ for odd modes). We set $j_{\rm max} = 12$ in this study.

Although even and odd modes are independent of each other, there is no pure dipole, or quadrupole mode since the pulsation energy is distributed among other values of ℓ_j because of the effects of the magnetic field. However, for convenience, we call a mode a distorted dipole mode if the $\ell_j = 1$ component is dominant, or a distorted quadrupole mode if the $\ell_j = 2$ component is dominant.

First, we choose a stellar model for the pulsation analysis. Table 2 lists observational parameters of HD 12098 adopted from the literature from which we also calculate the bolometric luminosity. Taking into account these parameters, we chose a $M = 1.75\,{\rm M}_\odot$ model having log(L/L$_\odot$) = 1.034 and log$T_{\rm eff}$(K) = 3.875 from the evolutionary models computed with the initial composition (X, Z) = (0.70, 0.02) in the fully ionized layers. The evolutionary models, common to our previous works (e.g. Holdsworth et al. 2016, 2018; Shi et al. 2021), were based on assumptions similar to the polar model of Balmforth et al. (2001), in which the helium mass fraction is depleted to 0.01 in the layers above the second He ionization zone to the surface, and convection in the envelope is neglected assuming a strong magnetic field to stabilize the outer layers.

Fig. 4 compares a dipole pulsation model ($\ell_0 = 1$) with the observed pulsational amplitude and phase modulations of HD 12098. For this model, we have chosen angles $\beta = 30^\circ$ and $i = 73^\circ$ to match the rotation phase at which sudden changes of the pulsation phases are seen. We have normalized the model amplitude to approximately fit the (secondary) maximum at a rotation phase of 0.15. At this phase the rotation axis, the line of sight and the magnetic axis are on a meridional plane with the visible magnetic pole at the angle (180°–β–i) from the line of sight. During the range of rotation phase between 0.0 and 0.3 (when the negative magnetic pole is seen in the lower part of the visible hemisphere) the amplitude and phase variations reasonably agree with those observed.

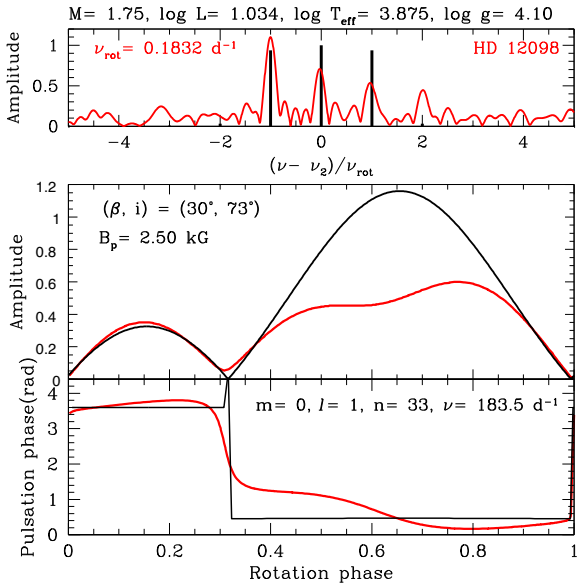

Figure 4. Comparison of observed Fourier amplitude (top), rotational modulations of the pulsation amplitude (middle), and the phase modulation (bottom) of HD 12098 with a 1.75 M$_\odot$ dipole pulsator model at a 2.5 kG magnetic field.

During the rotation phases between 0.3 and 1.0, the positive magnetic pole is visible. The angle between the visible pole and the line of sight attains minimum (i–β) at the rotation phase 0.65, when the predicted pulsation amplitude is maximum. However, the predicted amplitude during this range of rotation phase deviates considerably from the observed one. The observed amplitude variation is asymmetric with a bump and tends to be lower than the model prediction. In this range of rotation phase, the other positive magnetic pole is visible with angles between (i–β) and $\frac{\pi}{2}$ rad from the line of sight. The cause of the deviation, and in particular the cause of the broad bump in amplitude, is not clear. The pulsation phase of our model is constant during this phase interval, while the observed one gradually decreases, which is probably caused by the effect of rotation (neglected in this model) as discussed in Bigot & Kurtz (2011).

The deviation of the predicted amplitude variation from the observed one results in a lack of the fourth frequency component in the Fourier spectrum shown in the top panel of Fig. 4. Our model always predicts a triplet-dominated frequency spectrum for an odd-mode oscillation even if it is significantly affected by contributions from components with $\ell_j \geq 3$, because such contributions are mostly cancelled through the surface integration as discussed in Saio & Gautschy (2004). For this reason, the Fourier amplitude at $(\nu - \nu_2)/\nu_{\rm rot} = 2$ detected in the pulsation of HD 12098 cannot be explained by an axisymmetric odd mode. Some non-axisymmetric variation is needed for the Fourier component. In this respect, the bump in the amplitude modulation of HD 12098 might be caused by a non-axisymmetric (with respect to the magnetic axis) phenomenon and might be related with the Fourier component at $(\nu - \nu_2)/\nu_{\rm rot} = 2$.

Our model has a p-mode large separation of 5.47 d^{-1} (63.3 μHz) similar to the observational value ∼60 μHz. Fig. 5 compares model frequencies of distorted dipole and quadrupole p modes at $B_{\rm p}$ = 2.5 kG (upper panel) in the frequency range of HD 12098 (lower

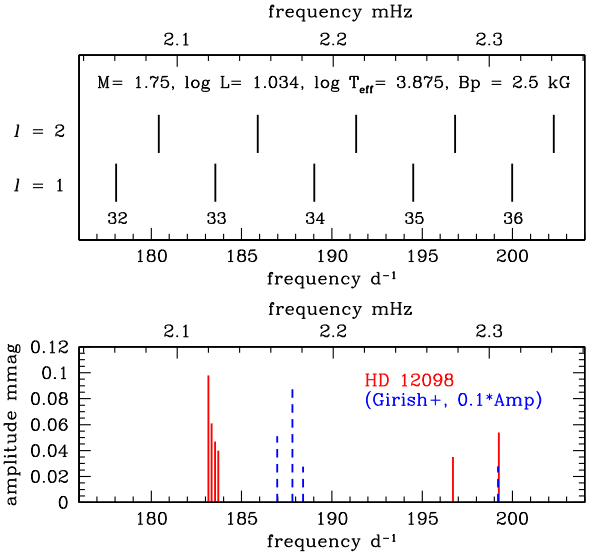

Figure 5. Comparison of observed frequencies with dipole and quadrupole modes of our model at $B_p = 2.5$ kG. The integer along each frequency of the dipole ($\ell = 1$) modes indicates the radial order. The dashed lines show the frequencies found by Girish et al. (2001) from ground-based Johnson *B* data.

panel). This figure indicates that the observed highest frequency ν_6 corresponds to the dipole mode of order 36, while ν_5 is the quadrupole mode of order 35. In addition, it is interesting to note that the frequency 189.2 d^{-1} (2.19 mHz) obtained by Martinez et al. (2000) is close to a dipole mode of order 34, one order higher than the order 33 for ν_2, indicating that the most strongly excited modes seem to shift with time, or that different modes are detected at different atmospheric depths (see Section 2.4 above). We do not know why the frequencies of highest amplitude found by Girish et al. (2001) do not match any of our model mode frequencies. We note, however, that these frequencies are all above the acoustic cut-off frequency, $\approx$135 d^{-1} (1.56 mHz), as in a number of other roAp stars (see fig. 12 of Holdsworth et al. 2018). The excitation mechanism for these high-frequency pulsations in roAp stars is not known.

Finally, we find that quadrupole modes [even modes ($\ell_0 = 0$) with the maximum amplitude at $\ell_j = 2$] affected with similar magnetic fields are not good for HD 12098. This is because the pulsational phase variations are significantly suppressed just as in our previous cases presented in, e.g. Holdsworth et al. (2016, 2018).

4 CONCLUSIONS

HD 12098 is an roAp star with a dipolar magnetic field and a rotation period of $P_{rot} = 5.460$ d. Using data from Sector 58 of the *TESS* mission, we have shown that there are rotational light variations consistent with spots, or patches, of enhanced abundances near to each of the magnetic poles. In these senses, HD 12098 is a typical α^2 CVn star.

HD 12098 is a known roAp star (Girish et al. 2001) for which the *TESS* data give far more insight to the pulsations than previous ground-based data. The star pulsates with several modes in the range 183–200 d^{-1} (2.12–2.31 mHz). While this encompasses the same frequency range found by Girish et al., the star has either changed modes, or the observations through the Johnson *B* bandpass and the *TESS* red bandpass sample different depths with different mode visibility. To discriminate between these possibilities requires simultaneous Johnson *B* and *TESS* observations.

The interesting new discovery for HD 12098 is that its principal pulsation mode is a dipole mode that is far more distorted than has been observed in other roAp stars. Using models that have reasonably explained the mode distortion in other roAp stars, we are unable to account for the double-humped pulsation amplitude modulation between rotation phases 0.3–1.0. This characteristic has not been observed in any other roAp star. On the dipole pulsation mode hemisphere seen with best aspect during those 0.3–1.0 rotation phases, the mode is strongly distorted from a simple dipole.

Interestingly, recently oblique pulsators have been discovered in close binary stars where dipole pulsations are strongly trapped in one hemisphere, or another – the tidally tilted pulsators and so-called single-sided pulsators (Fuller et al. 2020; Handler et al. 2020; Kurtz et al. 2020; Rappaport et al. 2021; Zhang et al. 2024). Whether the clear asymmetry of the pulsation in the dipole hemispheres of HD 12098 has any relation to this is unknown.

HD 12098 also shows a low-overtone p mode and possibly some g modes. These, too, are unusual in roAp stars and theoretically unexpected (Saio 2005) for this star's magnetic field strength of over a kG (Ryabchikova et al. 2005). This star calls for simultaneous multicolour photometric observations, and it presents new, challenging behaviour to theory.

ACKNOWLEDGEMENTS

DLH and DWK acknowledge support from the Fundação para a Ciência e a Tecnologia (FCT) through national funds (2022.03993.PTDC). This paper includes data collected by the *TESS* mission. Funding for *TESS* is provided by NASA's Science Mission Directorate. Resources used in this work were provided by the NASA High End Computing (HEC) Program through the NASA Advanced Supercomputing (NAS) Division at Ames Research Center for the production of the SPOC data products.

DATA AVAILABILITY

The *TESS* data used in this study are available on MAST.

REFERENCES

Ashoka B. N. et al., 2000, Bull. Astron. Soc. India, 28, 251
Balmforth N. J., Cunha M. S., Dolez N., Gough D. O., Vauclair S., 2001, MNRAS, 323, 362
Bigot L., Dziembowski W. A., 2002, A&A, 391, 235
Bigot L., Kurtz D. W., 2011, A&A, 536, A73
Crawford D. L., 1979, AJ, 84, 1858
Cunha M. S. et al., 2019, MNRAS, 487, 3523
Freyhammer L. M., Kurtz D. W., Elkin V. G., Mathys G., Savanov I., Zima W., Shibahashi H., Sekiguchi K., 2009, MNRAS, 396, 325
Fuller J., Kurtz D. W., Handler G., Rappaport S., 2020, MNRAS, 498, 5730
Gaia Collaboration, 2016, A&A, 595, A2
Gaia Collaboration, 2023, A&A, 674, A1
Girish V. et al., 2001, A&A, 380, 142
Handler G. et al., 2006, MNRAS, 366, 257
Handler G. et al., 2020, Nat. Astron., 4, 684
Holdsworth D. L., Kurtz D. W., Smalley B., Saio H., Handler G., Murphy S. J., Lehmann H., 2016, MNRAS, 462, 876
Holdsworth D. L., Saio H., Bowman D. M., Kurtz D. W., Sefako R. R., Joyce M., Lambert T., Smalley B., 2018, MNRAS, 476, 601
Holdsworth D. L. et al., 2024, MNRAS, 527, 9548
Jayaraman R., Handler G., Rappaport S. A., Fuller J., Kurtz D. W., Charpinet S., Ricker G. R., 2022, ApJ, 928, L14
Joshi S., Mary D. L., Martinez P., Kurtz D. W., Girish V., Seetha S., Sagar R., Ashoka B. N., 2006, A&A, 455, 303

Joshi S., Mary D. L., Chakradhari N. K., Tiwari S. K., Billaud S., 2009, AAP, 507, 1763
Joshi S. et al., 2016, A&A, 590, A116
Kochukhov O., 2006, A&A, 446, 1051
Kurtz D. W., 1982, MNRAS, 200, 807
Kurtz D. W., 1985, MNRAS, 213, 773
Kurtz D. W., Shibahashi H., Goode P. R., 1990, MNRAS, 247, 558
Kurtz D. W., Elkin V. G., Mathys G., 2006, in Fletcher K., Thompson M., eds, ESA SP-624: Beyond the spherical Sun. ESA, Noordwijk, p. 33
Kurtz D. W. et al., 2011, MNRAS, 414, 2550
Kurtz D. W. et al., 2020, MNRAS, 494, 5118
Kurtz D. W., Holdsworth D. L., 2020, in Monteiro M. J. P. F. G., García R. A., Christensen-Dalsgaard J., McIntosh S. W., eds, Astrophysics and Space Science Library, Vol. 57, Dynamics of the Sun and Stars; Honoring the Life and Work of Michael J. Thompson. Springer-Verlag, Berlin, p. 313
Martinez P. et al., 2000, Inf. Bull. Var. Stars, 4853, 1
Martinez P. et al., 2001, A&A, 371, 1048
Medupe R., Kurtz D. W., 1998, MNRAS, 299, 371
Medupe R., Kurtz D. W., Elkin V. G., Mguda Z., Mathys G., 2015, MNRAS, 446, 1347
Netopil M., Paunzen E., Maitzen H. M., North P., Hubrig S., 2008, A&A, 491, 545
Olsen E. H., 1983, A&AS, 54, 55
Quitral-Manosalva P., Cunha M. S., Kochukhov O., 2018, MNRAS, 480, 1676
Rappaport S. A. et al., 2021, MNRAS, 503, 254
Ryabchikova T. et al., 2005, A&A, 429, L55
Saio H., 2005, MNRAS, 360, 1022
Saio H., Gautschy A., 2004, MNRAS, 350, 485
Shi F., Kurtz D. W., Holdsworth D. L., Saio H., Cunha M. S., Zhang H., Fu J., Handler G., 2021, MNRAS, 506, 5629
Shibahashi H., Saio H., 1985, PASJ, 37, 245
Shibahashi H., Takata M., 1993, PASJ, 45, 617
Takata M., Shibahashi H., 1994, PASJ, 46, 301
Takata M., Shibahashi H., 1995, PASJ, 47, 219
Wade G. A., Bagnulo S., Donati J. F., Lueftinger T., Petit P., Sigut T. A. A., 2001, A Peculiar Newsletter 35, 35
Zhang V., Rappaport S., Jayaraman R., Kurtz D. W., Handler G., Fuller J., Borkovits T., 2024, MNRAS, 528, 3378

This paper has been typeset from a TEX/LATEX file prepared by the author.